Journal of
Synchrotron
Radiation

ISSN 0909-0495

Received 15 September 2008
Accepted 3 December 2008

The RATIO method for time-resolved Laue crystallography

Philip Coppens,[a]* Mateusz Pitak,[a] Milan Gembicky,[a] Marc Messerschmidt,[a] Stephan Scheins,[a] Jason Benedict,[a] Shin-ichi Adachi,[b,c] Tokushi Sato,[c,d] Shunsuke Nozawa,[c] Kohei Ichiyanagi,[c] Matthieu Chollet[d] and Shin-ya Koshihara[c,d,e]

[a]Chemistry Department, State University of New York at Buffalo, Buffalo, NY 14260-3000, USA, [b]High Energy Accelerator Research Organization, KEK, 1-1 Oho, Tsukuba, Ibaraki 305-0801, Japan, [c]Non-Equilibrium Dynamics Project, ERATO, Japan Science and Technology Agency, 1-1 Oho, Tsukuba, Ibaraki 305-0801, Japan, [d]Department of Materials Science, Tokyo Institute of Technology, 2-12-1-H61 Ohokayama, Meguro-ku, Tokyo 152-8551, Japan, and [e]Frontier Research Center, Tokyo Institute of Technology, 2-12-1 Ohokayama, Meguro-ku, Tokyo 152-8551, Japan. E-mail: coppens@buffalo.edu

A RATIO method for analysis of intensity changes in time-resolved pump–probe Laue diffraction experiments is described. The method eliminates the need for scaling the data with a wavelength curve representing the spectral distribution of the source and removes the effect of possible anisotropic absorption. It does not require relative scaling of series of frames and removes errors due to all but very short term fluctuations in the synchrotron beam.

Keywords: Laue diffraction; time-resolved diffraction; ratio method; data reduction.

1. Introduction

Time-resolved diffraction makes it possible to determine the structure of fleeting species, existing for microseconds or less, which may be crucial intermediates in photo-induced processes such as photochemical reactions and photo-generated electron transfer. Together with other techniques, including time-resolved UV–VIS spectroscopy, time-resolved electron paramagnetic resonance and time-resolved EXAFS, it offers the possibility of unprecedented insight in the progress of chemical and physical processes. Time-resolved studies of photo-induced processes have in common that a short light pulse is rapidly followed by an interrogating X-ray probe pulse. Variation of the time delay gives information on the progress of the process subject to study.

Monochromatic time-resolved (TR) diffraction at atomic resolution was initiated with the use of high-brightness radiation, as can be obtained at advanced synchrotron sources (Coppens *et al.*, 2005; Ozawa *et al.*, 2003; Hoshino *et al.*, 2006; Kim *et al.*, 2002). High brightness is essential as, owing to the mismatch between the rapid repeat of the synchrotron X-ray pulses (typically at a frequency larger than 1 MHz) and that of lasers with a sufficient power per pulse (typically <30 kHz), only a small fraction of the available X-ray photons can be used in the experiments. This means that to obtain sufficient counting statistics a stroboscopic experiment must be performed, in which the pump–probe cycle is repeated a large number of times while the counts are accumulated on an area detector. The 'light-on' intensities are then compared with those from a 'light-off' dark frame collected under identical conditions (except for the light) immediately after the 'on' frame.

While monochromatic methods for structure determination have the advantage of being highly accurate when conditions such as good crystal quality are fulfilled, there are several drawbacks for their use in time-resolved studies. First of all, the stroboscopic technique can only be applied to processes which are time-reversible on a rapid time scale, such as excitation to short-lived high-energy states. The technique requires that the crystal is subjected to a large number of rapidly repeating laser pulses, leading to specimen degradation and often resulting in several samples being needed in a single experiment. These are serious limiting disadvantages which dictate the search for practical alternatives, foremost among which is the polychromatic Laue technique, which has been applied successfully in relatively low-resolution macromolecular TR experiments (see, for example, Ren *et al.*, 2001; Bourgeois *et al.*, 2006; Anfinrud & Schotte, 2005; Anderson *et al.*, 2004), and makes much more efficient use of the available X-ray photons.

The RATIO method described in this article is based on analysis of the ratio of a pair of reflection intensities after exposure and before exposure. Earlier work based on the changes in intensity on chemical change and on light-induced changes are described by Hajdu *et al.* (1987) and Ren *et al.* (1996), respectively, as discussed further below.

2. Drawbacks of Laue diffraction in accurate crystallography

A dramatic difference between a frame of Laue data and a monochromatic frame is in the number of reflection spots that are observed. However, as the reflections that occur are generated in a range of wavelengths, reduction to a uniform set of structure factors requires knowledge of the spectral distribution of the incident beam and other wavelength-dependent effects such as absorption, anomalous scattering and the energy dependence of the detector response. In practice all wavelength-dependent effects are incorporated in a 'λ-curve', which in most programs, including the program *PRECOGNITION* (Ren *et al.*, 1999) used in the current study, is derived from the intensities of equivalent reflections collected several times at different wavelengths, and requires relative scaling of the frames in the data set. Use of a λ-curve based on a multi-frame data set implicitly assumes that the X-ray absorption in the crystal is isotropic. The final curve is obtained by a fitting procedure which in *PRECOGNITION* uses Chebyshev polynomials. In the 'pink' Laue technique the spectral distribution is that of a harmonic of the undulator. Unlike wiggler radiation used in earlier 'white' Laue synchrotron studies, which has a smoothly varying broad spectrum, this distribution is sharply peaked. An example is shown in Fig. 1. Though the result is pleasingly independent of the set of frames on which it is based, oscillations which may be dependent on the fitting procedure are evident.

An example of the scaling of both ON and OFF sets of frames is shown in Fig. 2. Though the results show the scale factors of the ON and OFF sets to have a closely related trend, differences between the two frames of an ON–OFF pair are too large to be acceptable when the response to light is to be evaluated. This difference and the uncertainty in the λ-curves indicates that alternative methods must be explored. Such a method is discussed in the following section.

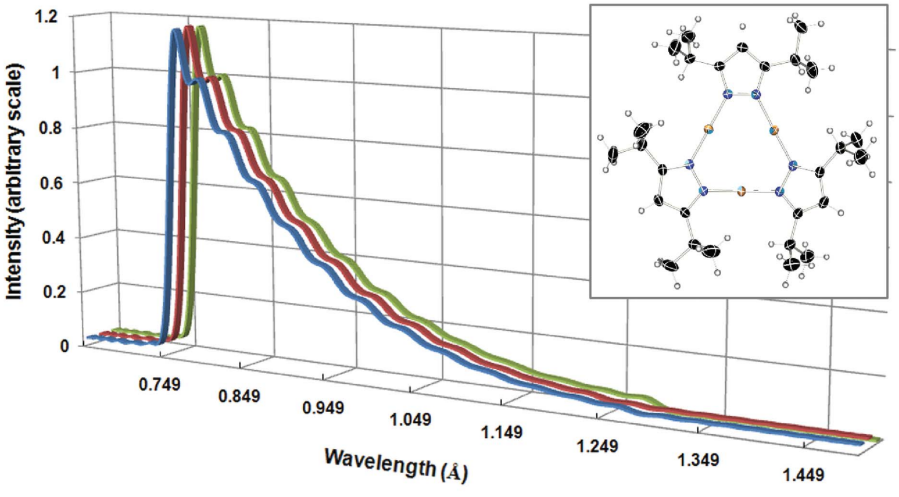

Figure 1
The λ-curve derived for a set of data on {[3,5-(*i*-propyl)$_2$pyrazolate]Cu}$_3$. Red: OFF frames only; green: ON frames only; blue: all frames. Numerical integration. Data collected at NW14, KEK, 13 mm undulator gap. The three curves essentially overlap, indicating that the result is not a function of the selection of the reflections.

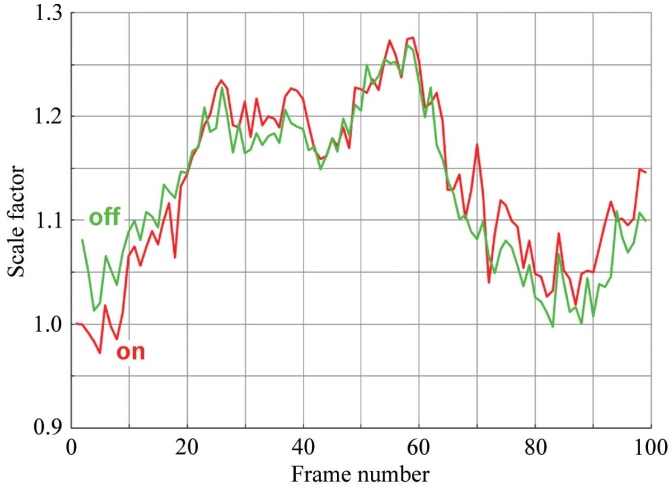

Figure 2
Scaling of ON and OFF frames for a set of data on $K_2MV[Pt_2(POP)_4]$ {MV = methylviologen, $Pt_2(POP)_4 = [Pt_2(H_2P_2O_5)_4]^{4-}$} (linear analytical integration). Data collected at NW14, KEK.

3. The RATIO method for Laue TR diffraction

The RATIO method is based on the direct combination of identical reflections on corresponding ON and OFF frames, which are collected within seconds from each other, and are thus unlikely to have different scale factors as would be implied by the curves shown in Fig. 2. The ON/OFF ratios R for each hkl from the different pairs of frames are subsequently averaged independent of the wavelength at which they are collected, implying the assumption that the relative effect of photo-induced changes is wavelength independent. We note that this assumption is not strictly valid if anomalous scattering effects significantly change the scattering power of certain atoms at specific wavelengths. It follows that the conditions must be selected such as to avoid inclusion of absorption edges in the wavelength range being employed in the experiments. If this is done, the RATIO method fully eliminates dependency on the λ-curve and its ambiguities.

In the method the ON/OFF ratios are treated as the observations, and repeatedly measured, and symmetry-related ratios are averaged using standard software, such as the program *SORTAV* (Blessing, 1997). If different data sets have been collected, consistency between data sets can be examined after singly measured ratios, or, more general, ratios only measured n times, n depending on the data set and the symmetry of the sample, are eliminated from the averaging. If the reproducibility is satisfactory, all ratios of each data set are included in a global averaging, but again excluding ratios occurring less than n times in the global

set. The ratios $R(hkl)$ can subsequently be combined with a monochromatic data set $I_{\rm OFF}(hkl)$, carefully collected at the same temperature as the TR experiment, to recover the $I_{\rm ON}$ intensities, using the expression

$$I_{\rm ON}(hkl) = I_{\rm OFF}(hkl)R(hkl) \quad (1)$$

or

$$F^2_{\rm ON}(hkl) = F^2_{\rm OFF}(hkl)R(hkl). \quad (2)$$

This step can be omitted if the refinement is based directly on the response ratios η, defined as $(I_{\rm on} - I_{\rm off})/I_{\rm off}$, as in the program *LASER* (Ozawa *et al.*, 1998; Vorontsov & Coppens, 2005), but the need for an OFF reference set of structure factors remains.

The theory of propagation of errors gives for the standard deviation in the $I_{\rm ON}/I_{\rm OFF}$ ratio R[1]

$$\sigma^2(R) = \sigma^2\big(I_{\rm ON}/I_{\rm OFF}\big) = \frac{1}{I^2_{\rm OFF}}\sigma^2\big(I_{\rm ON}\big) + \frac{I^2_{\rm ON}}{I^4_{\rm OFF}}\sigma^2\big(I_{\rm OFF}\big), \quad (3)$$

in which the standard deviations $\sigma(I_{\rm ON})$ and $\sigma(I_{\rm OFF})$ are those of the raw intensities, not affected by spectral corrections and scaling of the frames.

This gives, neglecting the errors in the monochromatic reference intensities,

$$\sigma\big(F^2_{\rm ON}\big) = \sigma(R)F^2_{\rm OFF}. \quad (4)$$

3.1. Comparison with related methods based on intensity changes

Hajdu *et al.* (1987) have analyzed intensity changes relative to a known starting set occurring on the binding of maltoheptose to glycogen phosphorylase. Data sets collected at different time points as the reaction progressed were scaled to the starting set to allow for beam decay, exposure time variations and radiation damage, to derive the relative intensity changes owing to the chemical reaction. As described above, the scaling step is omitted in the RATIO method, as the ON and OFF pairs are collected at time intervals of a few seconds and scaling between frames is omitted. In both procedures monochromatic data sets are used as reference.

In the 'relative change route' described by Ren & Moffat (1995), structure factor ratios are derived from the intensities of image plates exposed two or more times before and after laser illumination with different time delays, the image plate being translated between the exposures to prevent complete overlap of the reflections. The current method does not employ multiple exposures, but compares intensities on pairs of ON/OFF CCD frames, and is based on intensity ratios rather than ratios of the structure factors. Averaging of the intensity ratios of reflections measured several times and of symmetry-equivalents, collected in a series of experiments on different crystals, allows a test of the reproducibility of the measurements and the derivation of more reliable averaged response ratios. The squared structure factor ratios [expression (2)] are directly used as the observations in the subsequent least-squares refinement.

[1] $R = \eta + 1$.

3.2. Data collection

Data discussed in this report were collected at the NW14 station at the Photon Factory Advanced Ring (PF-AR) at the KEK synchrotron laboratory in Tsukuba, Japan (Nozawa *et al.*, 2007) and at the 14-ID station of BioCARS at the Advanced Photon Source (APS) at Argonne National Laboratory. They are referred to below as A (AR ring) and B (BioCARS). At A, X-ray pulses are generated by a single electron bunch of 60 mA occurring every 1.26 µs. The beam is not focused but truncated by a 250 × 250 µm aperture. At B, data collection used the single 15 mA m bunch of the hybrid APS mode, separated from other bunches by 1.59 µs. The X-ray beam was focused into a 125 × 125 µm spot shape to give a sufficient flux for single-pulse data collection. A frame of data collected with an undulator setting corresponding to a $\lambda_{\rm max}$ value of 12 keV is shown in Fig. 3. The pattern is of a salt of the photosensitizer cation $Cu(dmp)_2^+$ with a large counterion: $Cu(dmp)_2(TFPB)$ {$Cu(dmp)_2$ = Cu(I)(2,9-dimethyl-1,10-phenanthroline)$_2$; TFPB = tetrakis[3,5-bis(trifluoromethyl)phenyl] borate}.

At A, a pulse train of 10–20 pulses was used for data collection. The highly focused beam in the experiments conducted at B allowed collection of a frame of data with one single pulse (Fig. 3). The pump–probe delay in data sets collected at A was set at 200 ns.

At B, data frames on crystals of $Cu(dmp)_2(THPE)$ [$Cu(dmp)_2$ = Cu(I)(2,9-dimethyl-1,10-phenanthroline)$_2$; THPE = tris(4-hydroxyphenyl) ethane], in which the cation is embedded between hydrogen-bonded layers of anionic THPE (Zheng *et al.*, 2006), were collected with both 200 ps and 200 ns spacing between the pump and probe pulses. The peak energy of the undulator was set at 16 keV. The incident laser

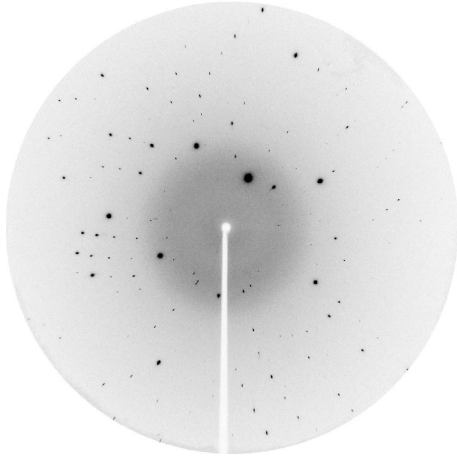

Figure 3
Laue diffraction pattern collected on a ~90 µm linear dimension sample of $Cu(dmp)_2(TFPB)$ {$Cu(dmp)_2$ = Cu(I)(2,9-dimethyl-1,10-phenanthroline)$_2$; TFPB = tetrakis[3,5-bis(trifluoromethyl)phenyl] borate} with a single X-ray pulse at beamline 14-B at APS. 12 keV peak undulator setting (12 mm gap).

Table 1
Summary of data sets on $Cu(dmp)_2(THPE)$.

Frames were collected at 2° intervals.

	Sample size (μm)	Laser power (μJ pulse^{-1})	Wavelength (nm)	Number of pulses	Number of frames
1	100 × 100 × 50	50	585	2	50
1a	As above	75	585	2	50
2	80 × 80 × 60	75	585	2	120
3	90 × 90 × 60	75	585	1	90
4	90 × 90 × 70	75	585	2	80

power was either 50 or 75 μJ pulse^{-1} at a wavelength of 585 nm generated by an OPA-tuned Ti:sapphire laser (Table 1). It is of interest that for the sample of $Cu(dmp)_2(THPE)$ the spot size was essentially unchanged after 200 ps, but considerably elongated at the 200 ns time point. The effect was fully reversible: after detector read-out lasting a few seconds the initial spot shape was recovered. Three successive exposures are shown Fig. 4. This effect was further investigated in experiments to be reported separately.

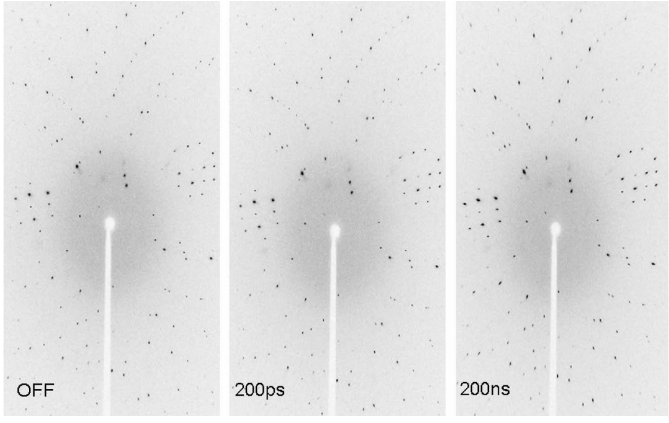

Figure 4
Three successive exposures of $Cu(dmp)_2(THPE)$ before laser illumination (left) and at time points of 200 ps (center) and 200 ns (right). Ti-sapphire laser with OPA tuned to 585 nm. ∼75 μJ pulse^{-1}, temperature 90 K.

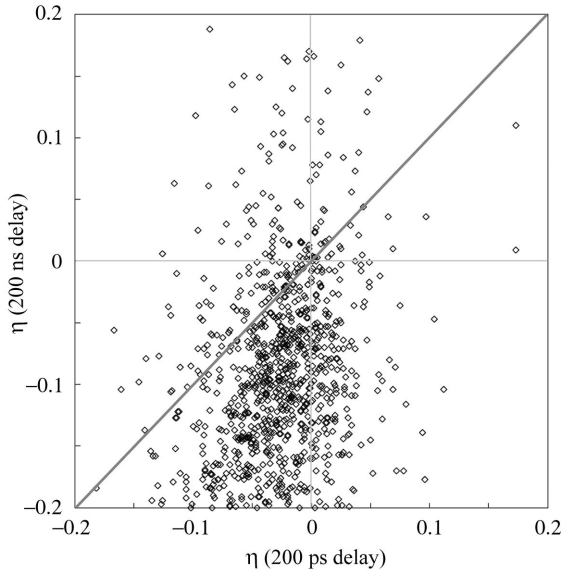

Figure 5
Correlation between response ratios η, defined as $(I_{on} - I_{off})/I_{off}$, at 200 ns and 200 ps obtained with the fixed elliptical integration in a single data set [$Cu(dmp)_2(THPE)$].

4. Application of the RATIO method

The RATIO method was tested on several data sets of different complexes. We discuss here five data sets collected on different samples of $Cu(dmp)_2(THPE)$ (see Table 1). The ON/OFF ratios measured were generally small and mostly in the 0.75–1.20 range. Weaker reflections with intensity less than 5σ were omitted from the analysis as the resulting standard deviations of the ratios were large. Even for the stronger reflections, the spread between equivalent measurements was considerably larger than predicted by the standard deviations based on statistics.

Several of the integration methods incorporated in the *PRECOGNITION* software were tested. Results reported here are based on fixed elliptical integration results, with the ellipsoid sizes carefully adjusted to incorporate the full area of the diffraction spots. When this was accomplished, a reasonable correlation between the response ratios of the corresponding individual reflections collected at 200 ps and 200 ns was obtained.

The data plotted in Fig. 5 show individual reflections before averaging over multiply measured reflections or symmetry equivalents. The 200 ns data show more negative response ratios, suggesting that the larger spot size was not fully accounted for in the integration procedure. As the Franck–Condon excitation and intersystem crossing are subpicosecond processes, use of a short time delay in excited-state geometry studies is indicated. Longer time delays can of course not be avoided if the course of a unidirectional reaction is to be studied.

In the next step of the analysis, repeatedly measured and symmetry-related reflections were averaged for each data set using the program *SORTAV* (Blessing, 1997). Reflections measured less than three times were omitted in this stage of the analysis to allow comparison between the different data sets collected on the same complex.

The correlation between equivalent reflections in different data sets is illustrated in Fig. 6. To obtain a final set of ratios, all 75 μJ pulse^{-1} data sets (1a, 2, 3, 4) were combined and averaged over repeated measurements and symmetry equivalents. Reflections occurring fewer than three times in the combined set were rejected. In this way any measurements occurring once or twice in individual sets, but repeatedly measured in different sets, can be included in the final analysis.

As expected, standard deviations in the final averaged set of ratios are considerably reduced compared with those in the individual sets and are typically 0.03–0.05. Nevertheless, the spread between ratios in different exposures evident in Figs. 5 and 6 indicates that integration techniques currently used in the analysis of Laue data must be re-examined before the

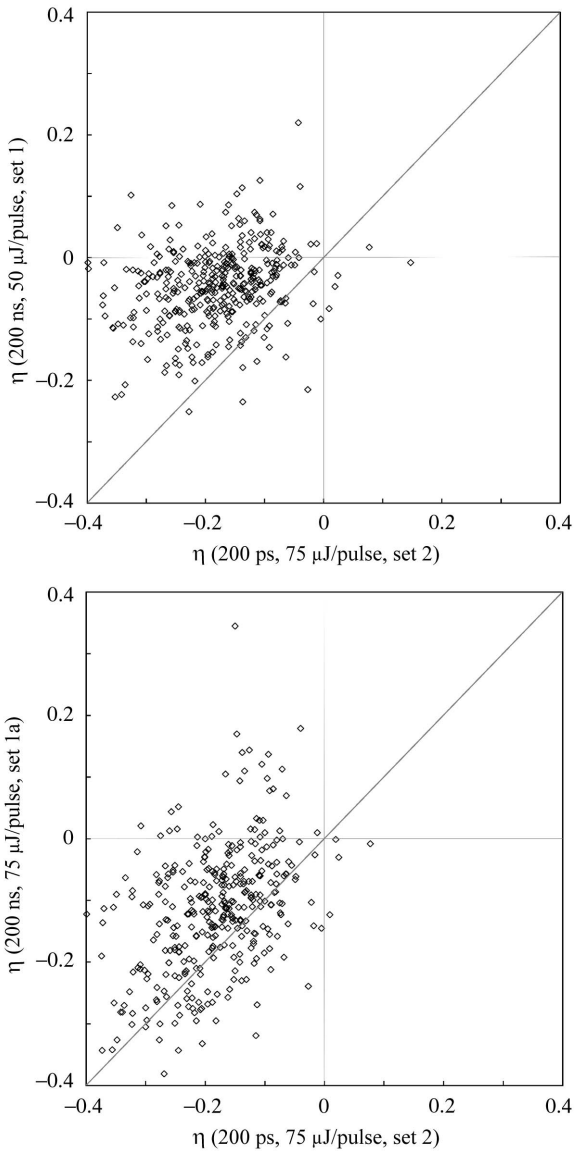

Figure 6
Evolution with time of the response ratios η, defined as $(I_{on} - I_{off})/I_{off}$. Fixed elliptical integration results. Top: run 1, collected at 50 μJ pulse^{-1} *versus* run 2, collected at 75 μJ pulse^{-1}. Bottom: run 1a *versus* run 2, both collected at 75 μJ pulse^{-1}, $I > 5\sigma$. Sample as in Fig. 5.

potential of the Laue technique in high-resolution time-resolved studies can be fully realised.

5. Conclusions

The RATIO method described here gives results independent of the wavelength dependence of the recorded reflection intensities, is independent of the assumption of isotropic absorption, and does not require relative scaling of the different frames. It thus eliminates a number of uncertainties inherent in the standard processing of Laue data. A remaining problem is the dependence of the reflection intensities on the various integration techniques available in the Laue software used, which requires additional attention.

Support of this work by the US Department of Energy (DE-FG02-02ER15372) is gratefully acknowledged. This work at KEK was performed under the approval of the Photon Factory Program Advisory Committee (Proposal No. 2004S1-001). We thank Dr Philip Anfinrud and his co-workers for expert assistance with the experiments at beamline 14-ID at the Advanced Photon Source, and Dr Vukica Šrajer for helpful discussions. Use of the BioCARS Sector 14 was supported by the National Institutes of Health, National Center for Research Resources, under grant number RR007707.

References

Anderson, S., Srajer, V., Pahl, R., Rajagopal, S., Schotte, F., Anfinrud, P., Wulff, M. & Moffat, K. (2004). *Structure*, **12**, 1039–1045.
Anfinrud, P. & Schotte, F. (2005). *Science*, **309**, 1192–1193.
Blessing, R. H. (1997). *J. Appl. Cryst.* **30**, 421–426.
Bourgeois, D., Vallone, B., Arcovito, A., Sciara, G., Schotte, F., Anfinrud, P. A. & Brunori, M. (2006). *Proc. Natl. Acad. Sci.* **103**, 4924–4929.
Coppens, P., Vorontsov, I. I., Graber, T., Gembicky, M. & Kovalevsky, A. Y. (2005). *Acta Cryst.* A**61**, 162–172.
Hajdu, J., Machin, P. A., Campbell, J. W., Greenhough, T. J., Clifton, I. J., Zurek, S., Gover, S., Johnson, L. N. & Elder, M. (1987). *Nature (London)*, **329**, 178–181.
Hoshino, M., Uekusa, H. & Ohashi, Y. (2006). *Bull. Chem. Soc. Jpn*, **79**, 1362–1366.
Kim, C. D., Pillet, S., Wu, G., Fullagar, W. K. & Coppens, P. (2002). *Acta Cryst.* A**58**, 133–137.
Nozawa, S. *et al.* (2007). *J. Synchrotron Rad.* **14**, 313–319.
Ozawa, Y., Pressprich, M. R. & Coppens, P. (1998). *J. Appl. Cryst.* **31**, 128–135.
Ozawa, Y., Terashima, M., Mitsumi, M., Toriumi, K., Yasuda, N., Uekusa, H. & Ohashiy, Y. (2003). *Chem. Lett.* **32**, 62–63.
Ren, Z., Bourgeois, D., Helliwell, J. R., Moffat, K., Šrajer, V. & Stoddard, B. L. (1999). *J. Synchrotron Rad.* **6**, 891–917.
Ren, Z. & Moffat, K. (1995). *J. Appl. Cryst.* **28**, 461–481.
Ren, Z., Ng, K., Borgstahl, G. E. O., Getzoff, E. D. & Moffat, K. (1996). *J. Appl. Cryst.* **29**, 246–260.
Ren, Z., Perman, B., Šrajer, V., Teng, T.-Y., Pradervand, C., Bourgeois, D., Schotte, F., Ursby, T., Kort, R., Wulff, M. & Moffat, K. (2001). *Biochemistry*, **40**, 13788–13801.
Vorontsov, I. I. & Coppens, P. (2005). *J. Synchrotron Rad.* **12**, 488–493.
Zheng, S.-L., Gembicky, M., Messerschmidt, M., Dominiak, P. M. & Coppens, P. (2006). *Inorg. Chem.* **45**, 9281–9289.